Available online on 15.03.2019 at http://jddtonline.info

Journal of Drug Delivery and Therapeutics

Open Access to Pharmaceutical and Medical Research

Open Access Research Article

Formulation by Design (FbD) approach to develop Tenofovir Disoproxil Fumarate loaded Nanostructured Lipid Carriers (NLCs) for the aptness of nose to brain delivery

Anupam Sarma [a,b], Malay K. Das [a]

[a] Department of Pharmaceutical Sciences, Dibrugarh University, Dibrugarh, 786004

[b] Pratiksha Institute of Pharmaceutical Sciences, Guwahati, 781026

ABSTRACT

The objective of the present investigation was to optimize and develop Tenofovir Disoproxil Fumarate (TDF) loaded Nanostructured Lipid Carriers (NLCs) with Compritol 888 ATO as solid lipid and Oleic acid as liquid lipid by modified emulsion solvent diffusion method using Central Composite Design (CCD). Three independent variables viz., Lipid to Drug ratio (A), Aqueous phase pH (B) and Sonication time (min) (C) were taken to investigate their effect on dependent variables viz., particle size (nm) (R1), PDI (R2) and % Entrapment Efficiency (%EE) (R3). Optimized formula of NLC was selected from the design space which was further optimized by changing the surfactants quantity. NLCs were evaluated for physicochemical, morphological, solid state characterization, and in-vitro dissolution in PBS pH 6.4, PBS pH 7.4 and ACSF. The average particle size was found to be 94.7 ± 15.70 nm with PDI of 0.380 ± 0.024 and 134.3 ± 9.71 nm with PDI of 0.358 ± 0.038 respectively for T4 and T5 NLC formulation. The zeta potential value of -17.0± 3.87 mV and -17.17 ± 1.05 mV and %EE of 35.5 ± 1.04 % and 34.2 ± 2.78 %. Overall, the above finding shows promising results in the area of developing non-invasive intranasal route as an alternative to oral route for brain delivery.

Keywords: Central composite design, Intranasal, Neuro-AIDS, CNS targeting.

Article Info: Received 24 Jan 2019; Review Completed 26 Feb 2019; Accepted 03 March 2019; Available online 15 March 2019

Cite this article as:

Sarma A, Das MK, Formulation by Design (FbD) approach to develop Tenofovir Disoproxil Fumarate loaded Nanostructured Lipid Carriers (NLCs) for the aptness of nose to brain delivery, Journal of Drug Delivery and Therapeutics. 2019; 9(2):148-159 http://dx.doi.org/10.22270/jddt.v9i2.2391

***Address for Correspondence:**

Malay K. Das, Department of Pharmaceutical Sciences, Dibrugarh University, Dibrugarh, 786004

INTRODUCTION

In 1981, Acquired Immune Deficiency Syndrome (AIDS) was first detected as a new disease when unusual opportunistic infections and rare malignancies were observed among young homosexual men [1], and its causative organism human immunodeficiency virus (HIV) was discovered in the year 1983 [2]. But, till today, AIDS is a chronic and often fatal disease of pandemic proportions. HIV infection results in cell-mediated immune deficiency through progressive loss and dysregulation of CD4+ T lymphocytes, leading to AIDS [3]. When HIV was initially isolated and characterized, it was believed to infect only CD4 lymphocyte, and the effects were restricted to the suppression of the immune system. However, in 1985, HIV was recovered from brain tissue, spinal cord, and peripheral nerves of the patient. This observation provided evidence of the role of HIV in causing primary infection of the brain [4]. HIV directly infects and injure both systemic and innate, central and peripheral nervous systems, immune systems through infection respectively of T-helper lymphocytes and of microglia, culminating in a wide spectrum of neuropsychiatric disorders or neuroAIDS. NeuroAIDS is associated with neurocognitive disorders such as HIV-associated dementia, minor neurocognitive disorder, mania/psychosis, anxiety, depression, seizures, mental slowness, forgetfulness, poor concentration, discombobulation, speech problem, decrease in spontaneity, myelopathy, and neuropathy with accompanying chronic neuropathic pain and physical disabilities. [4, 5, 6]

Brain/CNS is a very complex system; it provides a natural defense against toxic or infective agents circulating in the blood [7]. The same mechanisms that protect the brain from foreign substances also restrict the entry of potentially active therapeutic moieties [8]. The CNS delivery of antiHIV drugs is limited by the blood–brain and blood–CSF interfaces due to a combination of restricted paracellular movement, powerful metabolic enzymes and numerous transporters including members of the ATP-binding cassette (ABC) and solute carrier (SLC) superfamilies [9]. The BBB is often the rate-

limiting factor in determining permeation of therapeutic drugs into the brain [10].

Tenofovir disoproxil fumarate (TDF), a prodrug of the nucleotide reverse transcriptase inhibitor, tenofovir (9-[9(R)-2-(phosphonomethoxy) propyl]adenine; PMPA). Tenofovir is an acyclic nucleotide analog with potent *in vitro* and *in vivo* antiretroviral activity. Despite its demonstrated antiviral potency, tenofovir has limited oral bioavailability in animals. Its prodrug form Tenofovir disoproxil fumarate is well absorbed due to the presence of disoproxil moiety. The oral bioavailability of tenofovir from tenofovir DF is 25%. Once in the circulation, tenofovir is rapidly liberated and can be absorbed into cells where cellular enzymes directly produce the active metabolite, tenofovir diphosphate. Tenofovir diphosphate competitively inhibits human immunodeficiency virus (HIV) reverse transcription and causes chain termination of the nascent viral cDNA. Tenofovir is primarily eliminated renally as unchanged drug with active tubular secretion by the kidney. The terminal half-life of tenofovir approximately 11-14 hours. There is the negligible transport of tenofovir across the blood-brain barrier [9, 11, 12, 13].

The blood–brain barrier (BBB) prevents drugs permeability into the brain and limits the management of brain diseases. Intranasal delivery is a convenient route of drug administration that can bypass the BBB and lead to a direct delivery of the drug to the brain due to unique relationship between nasal cavity and cranial cavity and transported via the olfactory epithelium and/or via the trigeminal nerves directly to the CNS (Figure 1 & Figure 2). Indeed, drug accumulation in the brain following intranasal application of a drug solution, or of a drug encapsulated in specialized delivery systems (DDSs), has been reported in numerous scientific publications.[14, 15, 16] Various patents are also granted for delivery of bupropion, folic acid, mecamylamine, modafinil etc to brain through intranasal route. [17, 18, 19, 20]

Colloidal drug carriers offer a number of potential advantages for drug delivery. Lipid nanoparticles (LNPs) have attracted special interest during last few decades. Solid lipid nanoparticles (SLNs) and nanostructured lipid carriers (NLCs) are two major types of Lipid-based nanoparticles. SLNs were developed to overcome the limitations of other lipidic nanocarriers, such as emulsions, liposomes, and polymeric nanoparticles because they have advantages like good release profile and targeted drug delivery with excellent physical stability. In the next generation of the lipid nanoparticle, the presence of solid cum liquid lipid in the NLC leads to greater drug encapsulation and loading and long-term colloidal stability. In SLN, it is observed that the drug amount soluble in the lipid melt before particle production is higher than in the final SLN and such higher drug concentration in the melt might result in immediate drug expulsion during the cooling process. In contrast, in NLC the solid matrix of the lipid nanoparticle contains a nano-oil section in which drug solubility is higher, thus increasing the total drug loading capacity. NLC exhibit a biphasic drug release pattern that is, an initial burst release of drug followed by a sustained release at a constant rate. The liquid lipid located in the outer layers of the nanoparticles forms drug-enriched casing which leads to burst release of the drug at the initial stage. The conception of NLC that is lipid matrices which are solid, but not crystalline is derived from the fact that crystallization process itself causes the expulsion of the drug. By using special mixtures of solid lipids and liquid lipids, the particles become solid after cooling but do not crystallize. NLC have easily stabilized with a minimum possible concentration of surfactants along with best results of stability, entrapment, and release. Sometimes, even 0.5-1% of the surfactant is sufficient for developing stable NLC [21, 22].

Compretol 888 ATO is chemically Glyceryl behenate an ester of glycerin with behenic acid. The latter is a long-chain saturated fatty acid (C22) that is found in small quantities in normal dietary components like dairy fats, fish oil, peanut oil and canola oil. Compritol 888 ATO is registered in both EP and USP. It is generally regarded as a relative nonirritant and nontoxic material. Glyceryl behenate is a fat used in cosmetics, foods, and oral pharmaceutical formulations. In cosmetics, it is mainly used as a viscosity-increasing agent in emulsions. In pharmaceutical formulations, it is mainly used as a tablet and capsule lubricant, as a lipidic coating excipient and matrix-forming agent for the controlled release of water-soluble drugs. It is also used widely as an ingredient for the preparation of lipidic nanoparticles such as solid lipid nanoparticles (SLN) and nanostructured lipid carriers (NLC) [23, 24].

Oleic acid consists chiefly of (Z)-9-octadecenoic acid together with varying amounts of saturated and other unsaturated acids. Oleic acid is included in the FDA Inactive Ingredients and it is generally regarded as a relative nonirritant and nontoxic material. Oleic acid is a fatty acid that occurs naturally in various animal and vegetable fats and oils. Oleic acid is the most abundant fatty acid in human adipose tissue. It has also been used as a penetration enhancer in transdermal formulations, to improve the bioavailability of poorly water-soluble drugs in tablet formulations. Oleic acid has also been tested in novel drug delivery system like NLC [25, 26].

Compritol 888 ATO and oleic acid both are found in various dietary foods. Both of these are fatty acid and degraded by oxidation in vivo and form acetyl-CoA (coenzyme A) which is entry molecule of the citric acid cycle for energy production. So NLC formulation with these two materials will be biocompatible and biodegradable, stable and can be easily scaled up as compared to other lipid formulations.

The present investigation is aimed to develop TDF loaded NLC system to have the potential of brain delivery via non-invasive intranasal route (IN). TDF loaded NLCs were formulated by Modified emulsion solvent displacement method and optimized using Response Surface Central Composite Design (CCD). The TDF loaded NLCs were evaluated for physicochemical, morphology, in-vitro drug release characteristics.

MATERIALS AND METHODS

Materials

TDF and Compritol ATO 888 were received as gift sample from Micro Labs Ltd. (Bangalore, India). Oleic acid, Pluronic F-68 and Tween 80 were purchased form Himedia (Mumbai, India). All other chemicals and reagents were of highly purified grade and were used without further purification.

Preparation of NLCs

The NLCs were prepared by modified emulsion solvent diffusion method. For this purpose, Oleic acid and Compritol 888 ATO were dissolved in ethanol with heating at 60ºC, which acts as lipid phase. Pluronic F-68 and Tween 80 were dissolved in water, which acts as aqueous phase. Preparation of NLC involves mixing of lipid phase with the aqueous phase at 60ºC. Prior to mixing both the phases were heated upto 60ºC [27]. The lipid phase was added drop-wise with the help of a syringe to the aqueous phase and stirred on a magnetic stirrer at 60ºC for 5 minutes. Sonication of the preparation was done in a bath sonicator at 60ºC. After that

the preparation was stirred on a magnetic stirrer until the temperature of preparation reduced to room temperature. TDF loaded NLCs were formulated by adding TDF into lipid phase which was added to aqueous phase and stirred on a magnetic stirrer. The obtained TDF-NLC suspension was filtered through Sephadex G-25 column to separate the NLCs from the unentrapped drug and freeze dried the TDF loaded NLCs using mannitol for further characterization.

Table 1: Formulation design as per CCD for the preparation of NLCs and their obtained responses

Run	Lipid : Drug	Aqueous phase pH	Sonication time (min)	Particle size (nm)	PDI	%EE	Zeta potential (mV)	%drug loading
1	2.5	10.02	15	334.6	0.28	38.92	-23.6	1.45
2	2.5	7.5	15	323.4	0.21	31.2	-26.9	1.11
3	2.5	7.5	6.59	362.7	0.23	28.2	-24	1.03
4	2.5	7.5	15	325.4	0.22	32.2	-25.9	1.21
5	2	6	20	311.8	0.16	21.95	-33	0.82
6	2	9	20	289.1	0.178	26.82	-25.2	0.98
7	3	9	20	310.2	0.21	38.89	-21.7	1.36
8	2.5	7.5	15	321.9	0.17	30.4	-28.9	1.10
9	2.5	7.5	15	322.3	0.16	29.8	-24.3	1.08
10	2	9	10	303.1	0.093	27.54	-25.3	0.99
11	2.5	7.5	15	326.2	0.21	30	-21.9	1.08
12	1.66	7.5	15	270.2	0.14	20.23	-24.2	0.79
13	2.5	7.5	23.41	314.7	0.31	29.5	-21.8	1.12
14	3	6	10	335.5	0.24	27.2	-27.9	1.11
15	2.5	4.98	15	330	0.24	20.2	-26	0.79
16	3	9	10	371.5	0.17	36.3	-24	1.32
17	2.5	7.5	15	325.8	0.28	31.3	-26.9	1.15
18	3	6	20	311.4	0.33	23.42	-25.2	0.88
19	2	6	10	351.6	0.24	22.12	-28.9	0.82
20	3.34	7.5	15	356.7	0.38	31.5	-25.3	1.17

Experimental design

A Response Surface Central Composite Design (CCD) was applied to investigate the effect of formulation variables on dependent variables and statistically optimize the formulation factors [28, 29]. The Lipid to Drug ratio (A), Aqueous phase pH (B) and Sonication time (min) (C) were selected as the factors and were accordingly varied. All the independent and dependent variables were mentioned in table 2. While Particle size (nm) (R1), PDI (R2) and %EE (R3) were selected as dependent variables/responses. Design-Expert software (Version 10.0.1, Stat-Ease Inc. USA) was employed for designing the experiment. Experimental design of different trial batches of NLCs and their responses were expressed in table 1. The optimized formulation batch was selected for further study.

Table 2: The independent and dependent variables and their levels in CCD.

Variables	Levels			Star points (α)	
	Low (-1)	Medium (0)	High (+1)	- α	+ α
Independent variables (factors)					
A - Lipid : Drug	2	2.5	3	1.66	3.34
B - Aqueous phase pH	6	7.5	9	4.98	10.02
C - Sonication time (min)	10	15	20	6.59	23.41
Dependent variables (response)					
R1 - Particle size (nm)	Minimize				
R2 - PDI	Minimize				
R3 – %EE	Maximize				

Optimization, data analysis, and desirability function

The NLC formulations were optimized by employing Design-Expert software using response surface methodology. As per the suggestion by the software, the polynomial model was selected which gave quadratic equations for all the response variables. Moreover, graphs were also generated by the Design-Expert software. The significance of these factors on the variable parameters was assessed by analysis of variance (ANOVA, 2-way). The results of ANOVA studies are shown in table *3*.

After the model fitting step, the optimization was done. During the optimization process, the all responses were considered to find out the formulation having the desired characteristics. The desirability function combines all the responses into one variable to predict the optimum levels for the independent variables. The desirability value of 0 represents an unacceptable value for the responses and a value of 1 represents the most desired value for the responses. In the end, the optimized formulation as suggested by the software was prepared and the parameters were compared to the expected values as given by the design.

Table 3: Summary of ANOVA results for response surface CCD of particle size, PDI and %EE

Response	Model	F value	P value	Inference
Particle size (nm)	quadratic	6.22	0.0043	Significant
PDI	quadratic	1.33	0.0330	Significant
%EE	quadratic	37.65	<0.0001	Significant

Effect of different concentrations of surfactants on the optimized formulation

The effect of different concentrations of different surfactants were observed using Pluronic F-68 and Tween 80 alone as well as combination of these two (Table 4) by changing the surfactants quantity in the optimized formulation. Further best two formulations were selected based on the particle size nearer to 100 nm, lower PDI, higher %EE and zeta potential around 15 to 25 mV.

Table 4: Formulation trials to see the effect of surfactants

Trial	Tween 80 (%w/w)	Pluronic F68 (%w/w)	Tween 80+Pluronic F68 (1:1) (%w/w)	Particle size (nm)	PDI	%EE	Zeta potential (mV)
T1	1.5	0	0	30.6	0.537	23.9	-6.31
T2	1	0	0	30.4	0.54	25.7	-10.8
T3	0.5	0	0	112.8	0.335	34.8	-13.6
T4	0	0	1.5	75.3	0.408	36.6	-18.1
T5	0	0	1	138.5	0.326	36.6	-24.5
T6	0	0	0.5	220.8	0.246	38.4	-21.2
T7	0	1.5	0	264.1	0.261	30.2	-24.3
T8	0	1	0	360.4	0.246	31.6	-25.6
T9	0	0.5	0	380	0.281	32.1	-20.4

Characterization of TDF loaded NLC

Particle size, PDI and zeta potential

Particle size and PDI of NPs were determined by dynamic light scattering (DLS) technique due to the Brownian motion of the particles using Particle size analyzer (Brookhaven Instrument Corporation, USA) while zeta potential was determined by Electophoretic Light Scattering (ELS) technique using a Zeta sizer ZS90, (Malvern Instrument Ltd., UK).

Percent drug-loaded (%DL) and percent encapsulation efficiency (%EE)

Percent encapsulation efficiency was determined by separating the unentrapped TDF from TDF-NLCs by using Sephadex G-25 column which acts on the principle of size exclusion chromatography. The absorbance of the unentrapped TDF was recorded spectrophotometrically at 260 nm

% DL and %EE were calculated using the following formula

$$\text{Percent Drug loaded (\%DL)} = \frac{\text{Weight of Drug in NLCs}}{\text{Weight of NLCs}}$$

$$\text{Percent Entraptment Efficiency(\%EE)} = \frac{\text{Total amount of Drug} - \text{Amount of unentraped Drug}}{\text{Total amount of Drug}}$$

Fourier transform infrared spectroscopy (FTIR)

The Fourier transform infrared (FT-IR) spectra of the of Compritol ATO 888, Oleic acid, Pluronic F-68, TDF, Tween 80 and NLCs were recorded on FTIR spectrophotometer (Bruker Alpha) in the range of 4000–400 cm^{-1}.

Differential scanning calorimetry (DSC)

Differential scanning calorimetric analysis was performed (PerkinElmer DSC 4000) to investigate the thermal and crystalline behaviour of Compritol ATO 888, Oleic acid, Pluronic F-68, TDF, Tween 80 and NLCs. A heating rate of 10ºC/min was employed in the range of 40–450ºC.

X-ray diffractometry (XRD)

Crystal characteristics of Compritol ATO 888, Pluronic F-68, TDF and NLCs were analyzed by powder X-ray diffraction (XRD) on (Bruker AXS D8 Focus). Scan parameters were set at 5s scan speed and increament at 0.02. A diffraction pattern in the range of 10–80º (2θ) was used at 25ºC.

Scanning electron microscopy (SEM)

The shape and surface characteristics of NLCs were determined by SEM (Zeiss Sigma) using gold sputter technique. Freeze dried NLCs were dusted onto a double sided tape on an aluminium stub. The stubs containing the sample were coated with gold. Photomicrographs were taken at the accelerated voltage of 5 KV.

Transmission electron microscopy (TEM)

The morphology of NLCs was observed under transmission electron microscope (FEI Tecnai G2 20 S-Twin) by using negative staining technique.

In vitro drug diffusion study

In vitro drug diffusion study was carried out using the dialysis bag method. Formulation equivalent to 1mg TDF was placed inside the bag, while 100 mL diffusion medium (PBS, pH 7.4, pH 6.4 and ACSF at 37ºC ± 1.0ºC) was kept in the receptor compartment under constant stirring during experiment. An aliquot of 1mL was withdrawn at predetermined time intervals and was replaced with drug

free medium and analyzed using UV spectrophotometer at 260 nm (SHIMADZU-UV). In vitro diffusion study was carried out for 48 h. To study the drug release mechanism, data were treated with various kinetic models. A diffusion stud1y for each formulation was carried out in triplicate.

RESULTS AND DISCUSSION

Statistical experimental design

The formulations were optimized using response surface central composite design. The Lipid to Drug ratio, Aqueous phase pH and Sonication time (min) were taken as factors and Particle size (nm), PDI and %EE were used as dependent variables. From the preliminary studies, the Lipid to Drug ratio was selected in the range of 2:1-3:1. Aqueous phase pH was kept in the range 6-9. Sonication time was found to be satisfactory in the range 10-20 min. In this way, under the experimental conditions studied, it was possible to establish the optimized formulation as that with Lipid to Drug ratio 2.18:1.00, Aqueous phase pH 9 and Sonication time at 20 min.

Influence of independent variables on the particle size

The effect on particle size (R1) was observed to be significant by ANOVA and the polynomial equation was found as follows:

Particle size (R1) = +510.37736 +21.62297*A -54.33643*B -2.65273*C +17.66667*A*B -1.58000*A*C -0.19000*B*C -19.68561*A^2 +0.77470*B^2 +0.16023*C^2

(Where A- Lipid to Drug ratio, B- Aqueous phase pH, C- Sonication time).

From the polynomial equation, it was observed that the Particle size decreases with decrease in Lipid to Drug ratio. Whereas increase in Aqueous phase pH and Sonication time results in decrease in particle size. The response surface graph is shown in *Figure 1*.

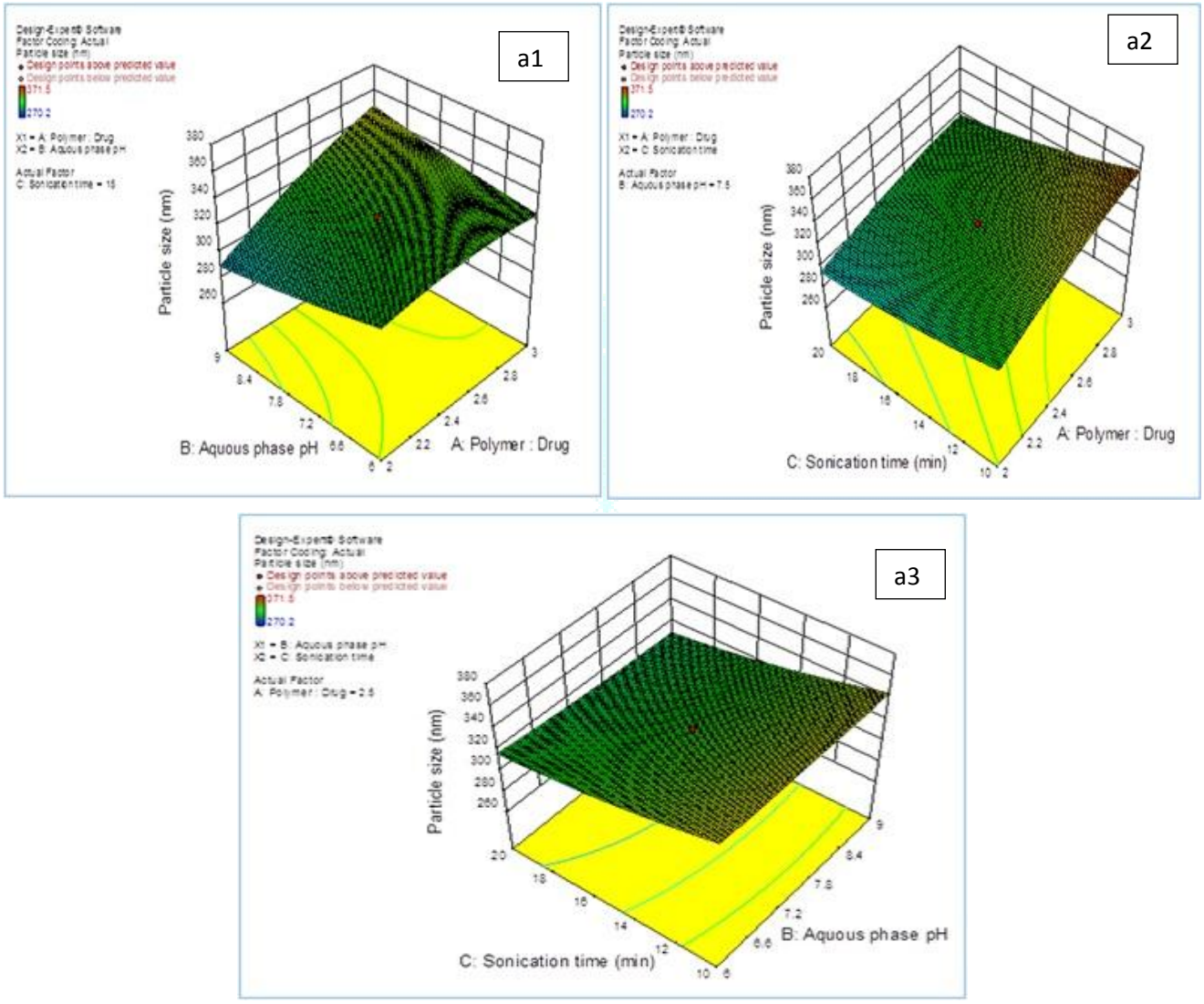

Figure 1: (a1) Response surface curves for particle size (effect of Aqueous phase pH and Lipid to Drug ratio). (a3) Response surface curves for particle size (effect of Sonication time and Aqueous phase pH). (a2) Response surface curves for particle size (effect of sonication time and lipid to drug ratio).

Influence of independent variables on PDI

The effect on PDI (R2) was observed to be significant by ANOVA and the polynomial equation was found as follows:

PDI = +0.56499 -0.012570*A -0.047301*B -0.035998*C -0.010167*A*B +0.006250*A*C +0.001917*B*C +0.019008*A^2 +0.002112*B^2 +0.000331*C^2

(Where A- Lipid to Drug ratio, B- Aqueous phase pH, C- Sonication time).

The polynomial equation shows that the PDI decreases with decrease in Lipid to Drug ratio, whereas Aqueous phase pH and Sonication time have no impact on it. The response surface graph is shown in *Figure 2*.

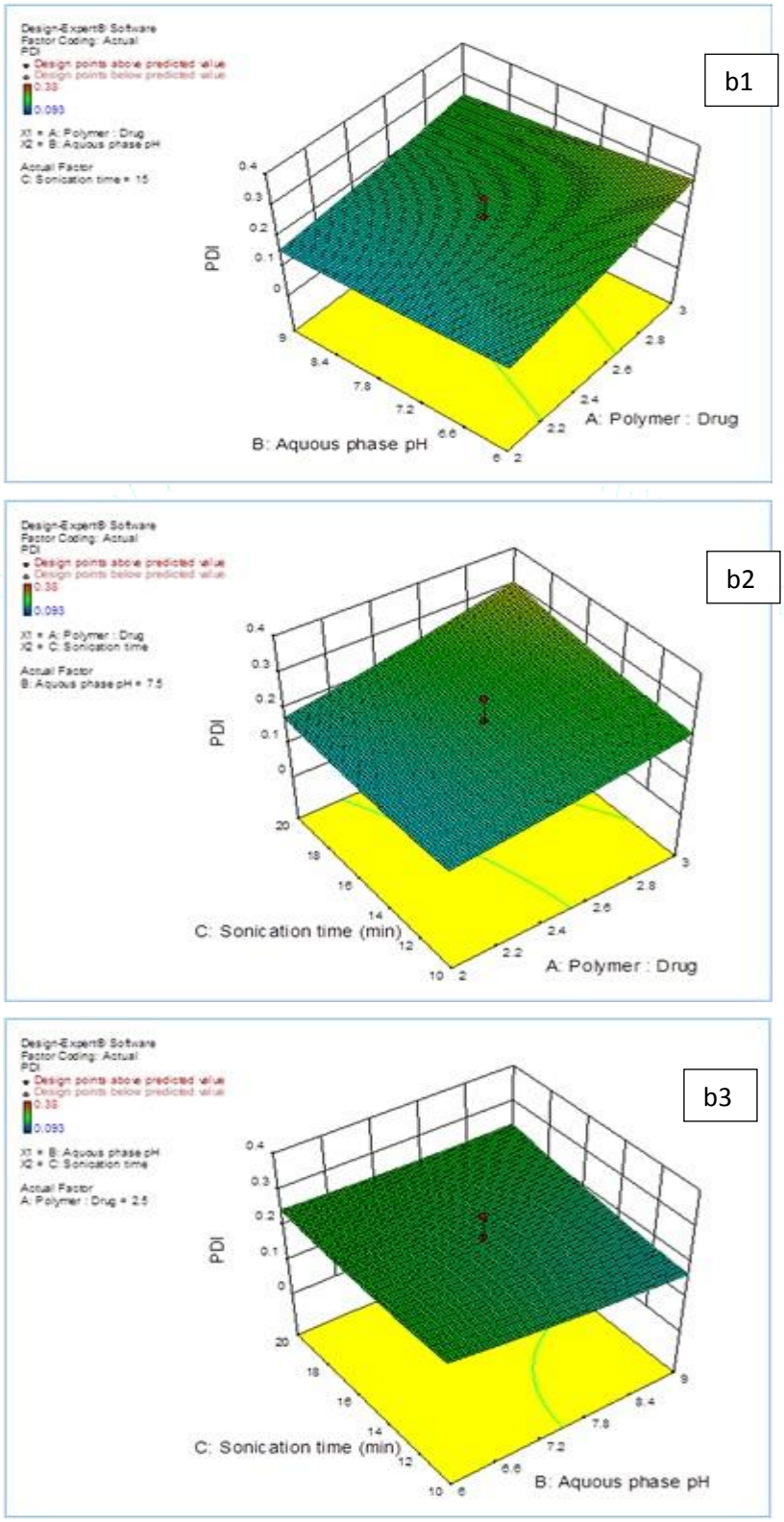

Figure 2:(b1) Response surface curves for PDI (effect of Aqueous phase pH and Lipid to Drug ratio). (b2) Response surface curves for PDI (effect of Sonication time and Lipid to drug ratio). (b3) Response surface curves for PDI (effect of Sonication time and Aqueous phase pH).

Influence of independent variables on % EE

The effect on % Cumulative drug permeation (R3) was similarly observed to be significant by ANOVA and the polynomial equation was found as follows:

% EE = -15.33000 +23.73662* A -1.35022*B +0.11970*C +2.38000*A*B -0.015000*A*C +0.097000*B*C -6.91524*A^2 -0.18775*B^2 -0.026938*C^2

(Where A- Lipid to Drug ratio, B- Aqueous phase pH, C- Sonication time).

From the equation, it is observed that % EE increases with increase in Lipid to Drug ratio and Aqueous phase pH. Whereas Sonication time don't have any effect on %EE. The response surface graph is shown in *Figure 3*

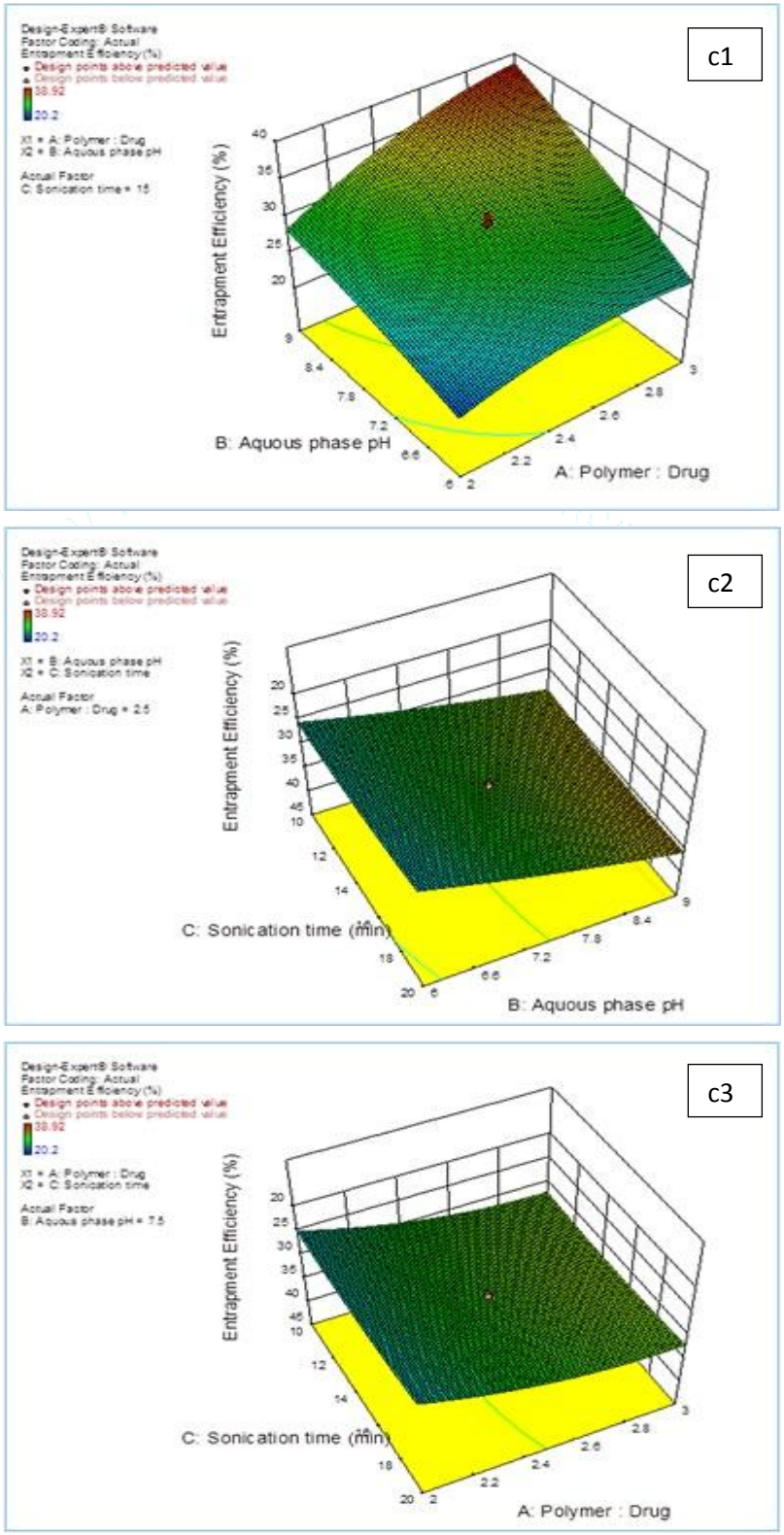

Figure 3:(c1) Response surface curves for %EE (effect of Aqueous phase pH and Lipid to Drug ratio). (c2) Response surface curves for %EE (effect of Sonication time and Aqueous phase pH). (c3) Response surface curves for %EE (effect of Sonication time and Lipid to drug ratio)

Formulation optimization using the desirability function

The aim of pharmaceutical formulation optimization is generally to find the levels of the variable that affect the chosen responses and determine the levels of the variable from which a robust product with high-quality characteristics may be produced. All the measured responses that may affect the quality of the product were taken into consideration during the optimization procedure. Upon "trading off" different response variables, the following criteria were adopted Lipid to Drug ratio, Aqueous phase pH, Sonication time were kept in the range. The responses of factorial formulations suggested a Lipid to Drug ratio 2.18:1.00, Aqueous phase pH 9 and Sonication time at 20 min as the optimized formulation.

Effect of different concentrations of surfactants on the optimized formulation

Effect of different concentrations of Tween 80, Pluronic F-68 and combination of these two on particle size, zeta potential and %EE were presented in *Table 4.* From the result it was seen that Teen 80 containing NLCs had lesser particle size compared to Pluronic F-68 composite NLCs. Whereas the NLCs containing combined Tween 80 and Pluronic F-68 at ratio 1:1 showed the intermediate particle sixe compared to the surfactants alone.

Characterization of NLCs

Particle size, PDI and zeta potential

Three individual formulations of optimized NLCs were formulated and characterized for size, PDI, zeta potential, %EE *(Table 5)*. Particle size measurements were required to confirm the production of particles in nano range. Particle size of T4 and T5 94.7 ± 15.70 nm with PDI of 0.380 ± 0.024 and 134.3 ± 9.71 nm with PDI of 0.358 ± 0.038 respectively indicated narrow size distribution with smaller size. Particle size is one of the major factor for intranasal delivery of drugs to the brain, because smaller the particle size larger the surface area thereby increased rate of drug absorption. At smaller size, higher amount of drug can be transported across the brain through olfactory region in nasal mucosa. Zeta potential is an electrical charge on the particle surface and acts as a factor for crossing biological membrane by the formulation. The zeta potential value of -17. ± 3.87 mV and -17.17 ± 1.05 mV was found for T4 and T5 respectively with %EE of 35.5 ± 1.04 and 34.2 ± 2.78.

Table 5: Characterization of T4 and T5 NLCs

Trial	Particle size (nm)	PDI	%EE	Zeta potential	%DL
T4	94.7 ± 15.70	0.380 ± 0.024	35.5 ± 1.04	-17.0 ± 3.87	1.22 ± 1.12
T5	134.3 ± 9.71	0.358 ± 0.038	34.2 ± 2.78	-17.17 ± 1.05	1.77 ± 0.89

Morphological analysis

SEM images representing surface morphology of NLCs are depicted in *Figure. 4.* NLCs were found to be spherical in shape with uniform distribution. SEM analysis revealed that the NLCs had smooth surface and did not show any aggregation. Morphological characteristic of the NLCs were analyzed using TEM *(Figure. 4).* It was observed that NLCs were spherical in shape.

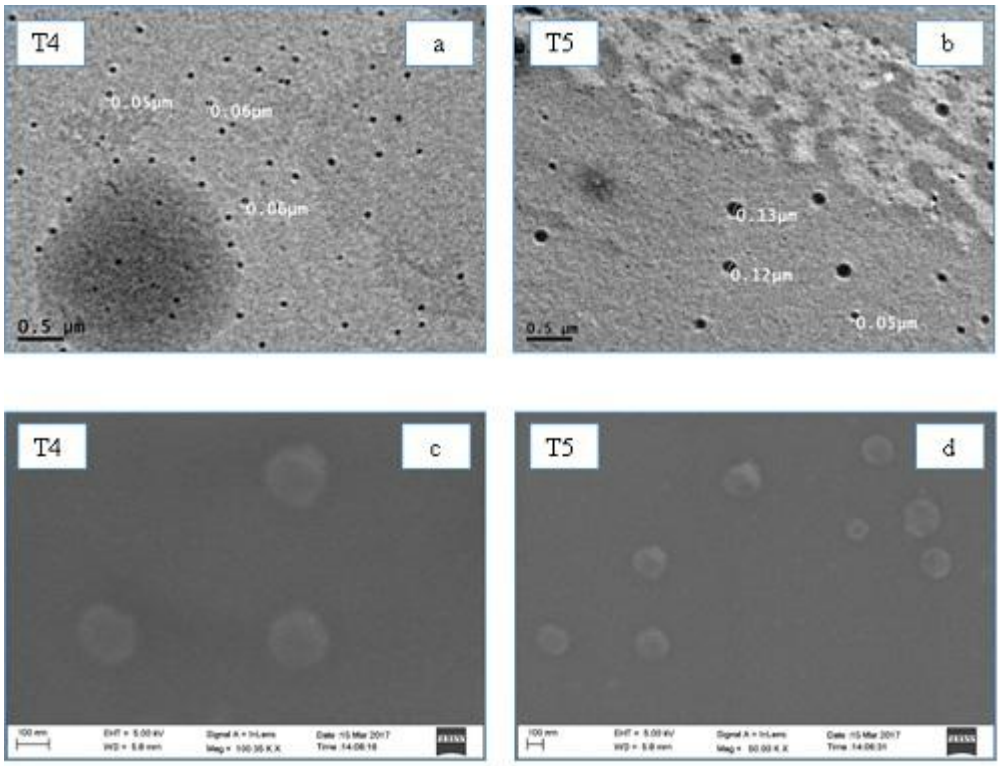

Figure 4: TEM image of T4 (a), T5 (b) and SEM image of T4 (c), T5 (d)

Fourier transform infrared spectra

The FTIR spectrum of TDF *(Figure 5)* exhibited sharp peak at 1752.29 cm^{-1} due to Carbonyl group stretching. The spectrum showed absorption band at 1622.33 cm^{-1} due to N-H bending, whereas the absorption band at 3227.13 cm^{-1} due to N-H stretching. The absorption band at 1256.26 cm^{-1} and 1680.37 cm^{-1} correspond to aromatic amine stretching and -C=N- stretching respectively. Absorption band at 1184.39 cm^{-1} confirms P=O stretching. The FTIR spectrum shows characteristic peaks of TDF Compritol ATO 888, Pluronic F68, Tween 80 and Oleic acid. In the IR spectrum of NLC (T4 and T5), major peaks corresponding to TDF are merged, disappear or are buried in the peaks of Compritol 888 ATO indicating drug entrapment in lipid matrix.

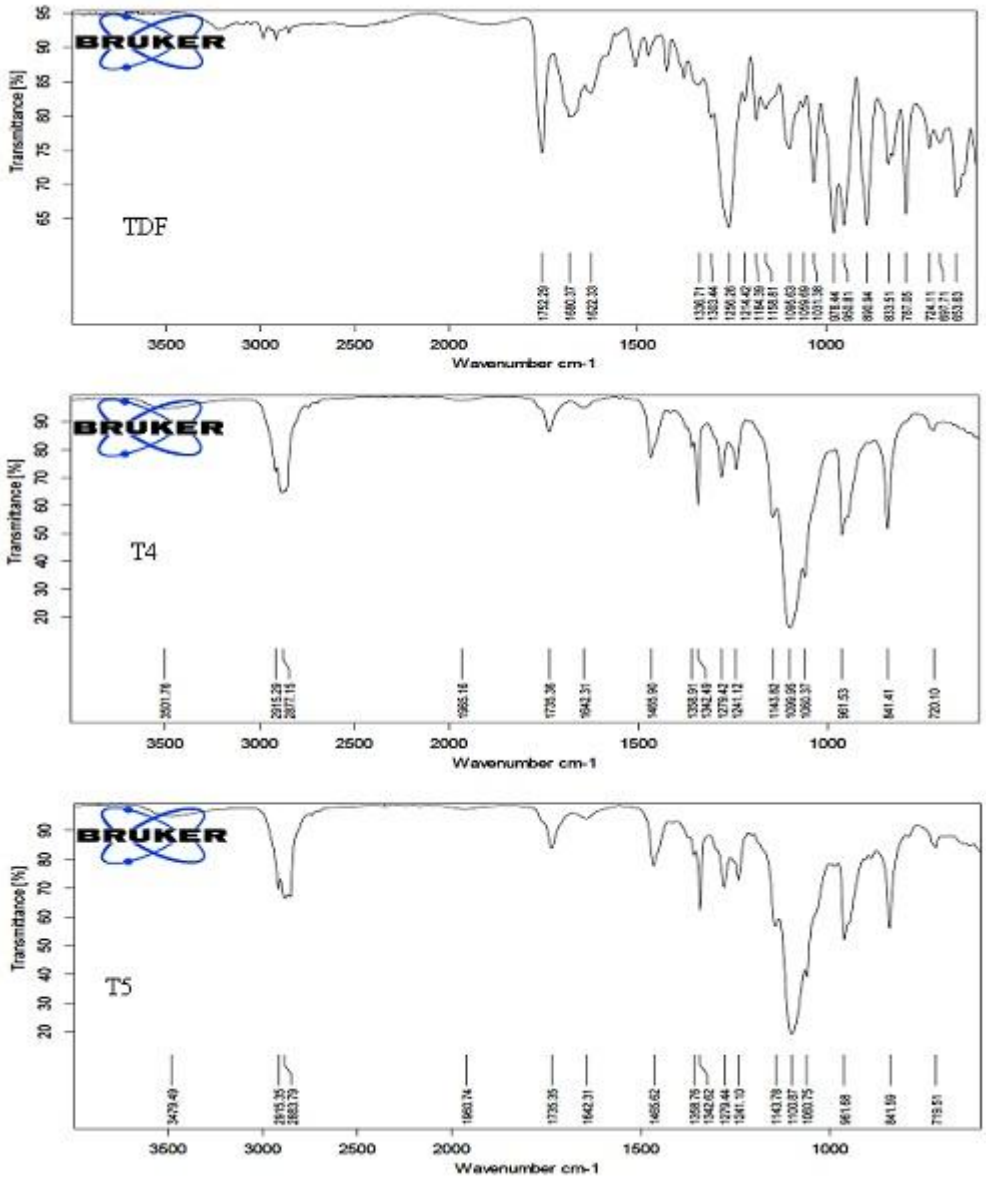

Figure 5: IR spectra of TDF, T4 and T5 NLCs

Differential scanning calorimetry

The DSC thermograms of TDF, Compritol ATO 888, Pluronic F68, Tween 80 and Oleic acid and NLCs were shown in *Figure 6*. Compritol ATO 888 thermogram showed endothermic peak at 78.53 ºC. Sharp melting endothermic peak of TDF was observed at 120.59 ˚C. The absence of characteristics endothermic peak of TDF in the DSC thermogram of NLCs might be because of formation of inclusion complex between hydrophobic cavities of Compritol ATO 888 and the drug in the NLCs.

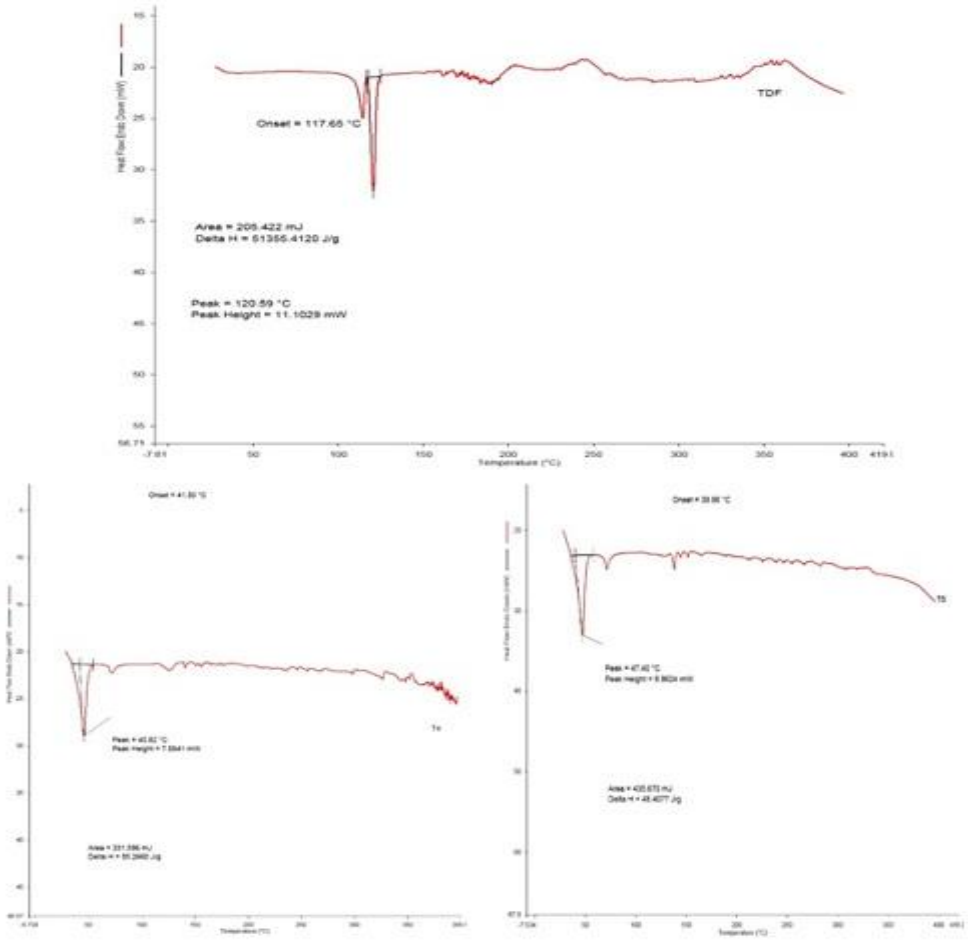

Figure 6: DSC thermogram of TDF, T4 and T5 NLCs

X-ray diffraction

Figure 7 shows XRD spectra of Compritol ATO 888, TDF, Pluronic F-68 and NLCs. XRD spectra of TDF, Compritol ATO 888 and Pluronic F68 shows some sharp peaks indicating its crystalline nature. From the spectra of NLCs it was observed that the XRD pattern of NLC also showed peaks for Compritol ATO 888 and Pluronic F68 indicating they were remained crystalline even in final NLC. The Sharp peaks of TDF were absent and/or showed very lower or negligible intensity in NLC indicating reduction in the crystallinity for TDF. It is known that, broadening and lowering of intensities observed in NLC compared to individual XRD spectra are characteristic of poor crystalline nature. This was because of entrapment of TDF within the NLC, thereby showing lower or negligible intensities for TDF in XRD spectra of NLCs.

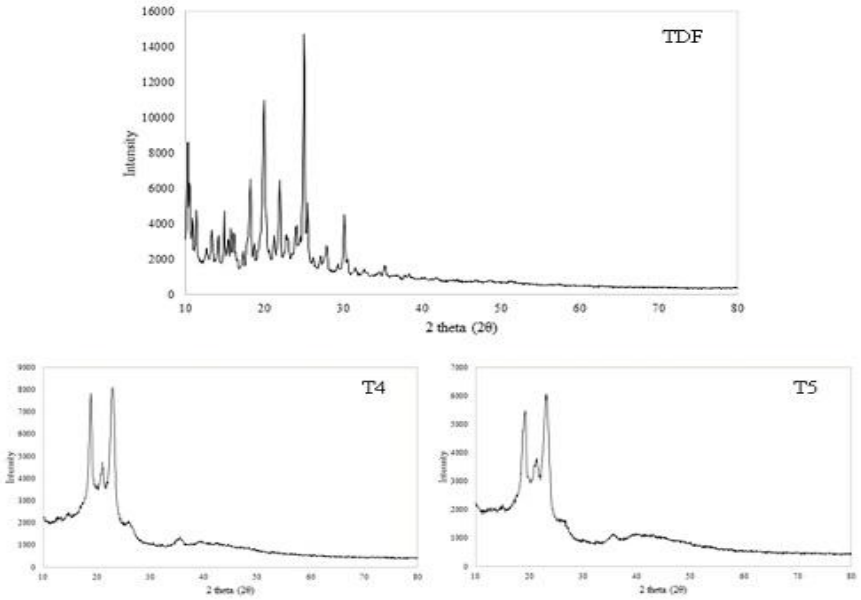

Figure 7: XRD of TDF, T4 and T5 NLCs

In vitro drug diffusion study

The release profile of TDF from the NLCs followed a biphasic pattern characterized by initial burst release followed by a slow prolonged release in all PBS pH 6.4, pH 7.4 and ACSF *(Figure 8, 9, 10).* The initial burst release may be attributed to the release of adsorbed drug molecules on the surface of NLCs in the diffusion media. Drug release was found to be sustained by erosion of polymer matrix which might have offered sustained release effect. Drug release profiles were analysed using zero order, first order, Higuchi, Hixon Crowell and Korsemeyer-Peppas model. The release exponent value (n) from the Korsemeyer–Peppas equation was found to be less than 0.5 which displayed drug release by Fickian diffusion mechanism with best correlation coefficient in all three dissolution medium viz. PBS pH 6.4, PBS pH 7.4 and ACSF.

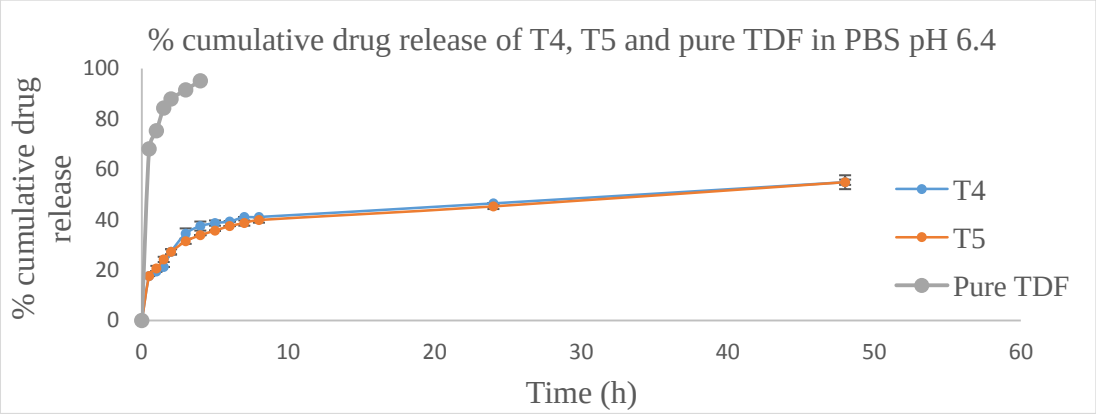

Figure 8: % cumulative drug release of T4, T5 and pure TDF in PBS pH 6.4

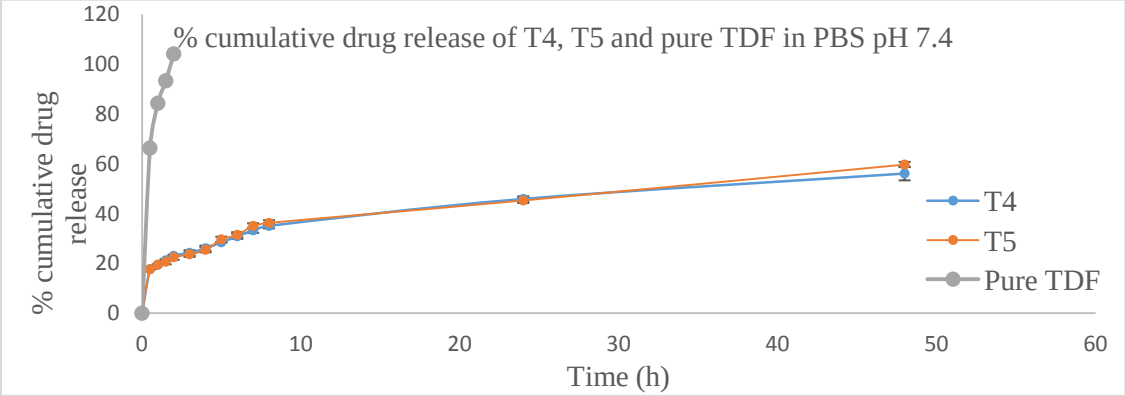

Figure 9: % cumulative drug release of T4, T5 and pure TDF in PBS pH 7.4

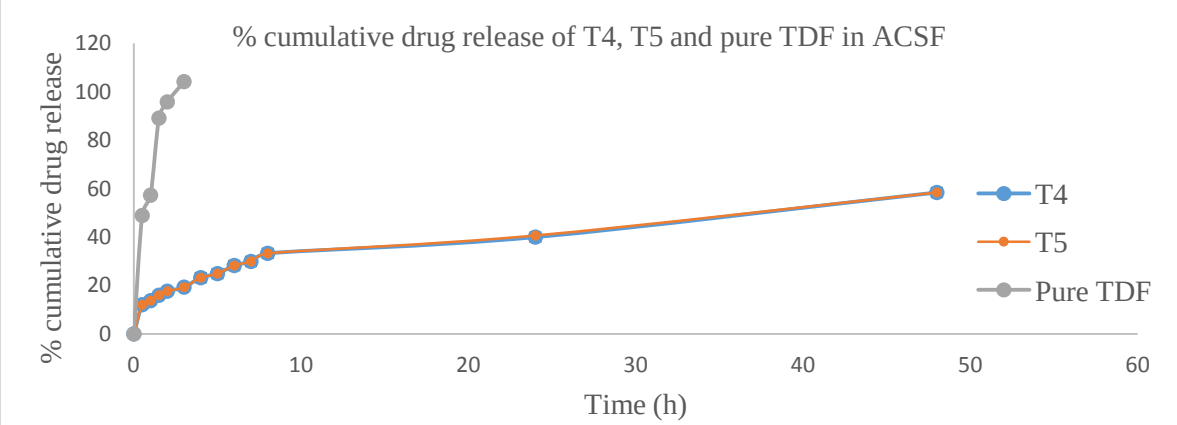

Figure 10: % cumulative drug release of T4, T5 and pure TDF in ACSF

CONCLUSION

In the present investigation CCD was successfully applied on the optimization and development of NLCs by modified emulsion solvent diffusion method. Design space was generated using CCD where three independent variables were taken to obtain optimized formula for NLCs with an aim to achieve lower size, PDI and higher %EE. Further the formula was again optimized by changing the surfactants which gave particle size of 94.7 ± 15.70 nm with PDI of 0.380 ± 0.024 and 134.3 ± 9.71 nm with PDI of 0.358 ± 0.038 respectively for T4 and T5 NLC formulation. Solid state characterization (DSC, FTIR and XRD) confirmed entrapment of TDF into NLCs successfully. Sustained release effect of TDF was observed from the NLCs in PBS pH 6.4, PBS pH 7.4 and ACSF. The low particle size with desired zeta potential for

NLCs proved the favourable effect on modulation of tight junctions of nasal cavity, thereby proving the potentiality of NLCs for the brain delivery via IN route in the area of therapeutic applications.

Acknowledgement:

We gratefully acknowledge the Department of Science and Technology (DST), Government of India, for providing a research grant through DST-UKIERI scheme (DST/INT/UK/P-88/2014).

REFERENCES

1. Paul MS, Beatrice HH. Origins of HIV and the AIDS pandemic. Cold Spring Harbor Perspect Med. 2011; 1:1–22.
2. Where did HIV come from? 2016; http://www.theaidsinstitute.org/node/259; Accessed 21 Sep 2016.
3. Friedrich BM, Dziuba N, Li G, Endsley MA, Murray JL, Ferguson MR. Host factors mediating HIV-1 replication. Virus Res. 2011; 161:101–14
4. Sharma D, Bhattacharya J. Cellular & molecular basis of HIVassociated neuropathogenesis. Indian J Med Res. 2009; 129:637–51
5. Bell JE, Anthony IC, Simmonds P. The changing pathology of NeuroAIDS associated with drug abuse in the era of HAART. Am J Infect Dis. 2006; 2: 39–48
6. McCombe JA, Noorbakhsh F, Buchholz C, Trew M, Power C. NeuroAIDS: a watershed for mental health and nervous system disorders. J Psychiatry Neurosci. 2009; 34:83–5
7. Peluffo H, Unzueta U, DemontelMLN, Xu Z, Váquez E, Miralles NF, et al. BBB-targeting, protein-based nanomedicines for drug and nucleic acid delivery to the CNS. Biotechnol Adv. 2015; 33:277–87
8. Grabrucker AM, Chhabra R, Belletti D, Forni F, Vandelli MA, Ruozi B, et al. Nanoparticles as Blood–Brain Barrier permeable CNS targeted drug delivery systems. TopicsMed Chem. 2004; 10:71–89
9. Varatharajan L and Thomas SA. The transport of antiHIV drugs across blood–CNS interfaces: Summary of current knowledge and recommendations for further research. Antiviral Research. 2009; 82(2):99–109.
10. Kaur IP, Bhandari R, Bhandari S, Kakkar V. Potential of solid lipid nanoparticles in brain targeting. J Control Release. 2008; 127:97–109
11. Anthonypillai C, Gibbs JE, Thomas SA. The distribution of the anti-HIV drug, tenofovir (PMPA), into the brain, CSF and choroid plexuses. Cerebrospinal Fluid Research. 2006; 3:1
12. Best BM, Letendre SL, Koopmans P, Rossi SS, Clifford DB, Collier AC, Gelman BB, Marra CM, McArthur JC, McCutchan JA, Morgello S, Simpson DM, Capparelli EV, Ellis RJ, Grant I, and the CHARTER Study Group. LOW CSF Concentrations of the Nucleotide HIV Reverse Transcriptase Inhibitor, Tenofovir. J Acquir Immune Defic Syndr. 2012; 59(4):376–381
13. Kozlovskaya L, Abou-Kaoud M, Stepensky D. Quantitative analysis of drug delivery to the brain via nasal route. J Controlled Release. 2014; 189:133–140
14. Selvamuthukumar S and Velmurugan R. Nanostructured Lipid Carriers: A potential drug carrier for cancer chemotherapy. Lipids in Health and Disease 2012; 11:159
15. Aburahma MH & Badr-Eldin SM. Compritol 888 ATO: a multifunctional lipid excipient in drug delivery systems and nanopharmaceuticals. Expert Opin. Drug Deliv. 2014; 11(12):1865-1883.
16. Bhavnaa, Shadab Md, Ali M, Ali R, Bhatnagar A, Baboota S, Ali J. Donepezil nanosuspension intended for nose to brain targeting:In vitro and in vivo safety evaluation. Int. J. Biol. Macromolec. 2014; 67:418–425
17. Shah B, Khunt D, Misra M, Padh H. Application of Box-Behnken design for optimization and development of quetiapine fumarate loaded chitosan nanoparticles for brain delivery via intranasal route. Int. J. Biol. Macromolec. 2016; 89:206–218
18. Alam MI, Baboota S, Ahuja S, Ali M, Ali J, Sahni JK, Bhatnagar. Pharmacoscintigraphic evaluation of potential of lipid nanocarriers for nose-to-brain delivery of antidepressant drug. Int. J. Pharm 2014; 470:99–106
19. Jung YS, Kim CS, Park HS , Sohn S , Lee BH , Moon CK , Lee SH , Baik EJ , and Moon CH. N-Nitrosocarbofuran Induces Apoptosis in Mouse Brain Microvascular Endothelial Cells (bEnd.3). J Pharmacol Sci. 2003; 93:489–495
20. Riss TL, Moravec RA, Niles AL, Duellman S, Benink HA, Worzella TJ, and Minor L. Cell Viability Assays. Assay Guidance Manual[Internet]. 2013. Last Update: July 1, 2016
21. Xu X, Khan MK, Burgess DJ. A quality by design (QbD) case study on liposomes containing hydrophilic API: II. Screening of critical variables, and establishment of design space at laboratory scale. Int. J. Pharm. 2012; 423:543– 553.
22. Singh S, Singh M, ripathi CB, Arya M & Saraf SA. Development and evaluation of ultra-small nanostructured lipid carriers: novel topical delivery system for athlete's foot. Drug Deliv. and Transl. Res. 2016; 6:38–47.
23. Kokatnur MG, Oalmann MC, Johnson WD, Malcom GT, Strong JP. Fatty acid composition of human adipose tissue from two anatomical sites in a biracial community. Am. J. Clin. Nutr. 1979; 32(11):2198–2205.
24. Gaba B, Fazil M, Khan S, Ali A, Baboota S, Ali J. Nanostructured lipid carrier system for topical delivery of terbinafine hydrochloride. Bulletin of Faculty of Pharmacy, Cairo University. 2015; 53:147–159
25. FDA Advisory Committee Briefing Document. http://www.fda.gov/ohrms/dockets/ac/01/briefing/3792b1_01_gilead.pdf]
26. Haque S, Md S, Sahni JK, Ali J, Baboota S. Development and evaluation of brain targeted intranasal alginate nanoparticles for treatment of depression. Journal of Psychiatric Research. 2014; 48:1-12
27. Shah B, Khunt D, Bhatt H, Misra M, Padh H. Application of quality by design approach for intranasal delivery of rivastigmine loaded solid lipid nanoparticles: effect on formulation and characterization parameters, Europian Journal of Pharmaceutical Science. 2015; 78:54–66
28. Beringhs AO, Rosa JM, Stulzer HK, Budal RM, and Sonaglio D. Green Clay and Aloe Vera Peel-Off Facial Masks: Response Surface Methodology Applied to the Formulation Design. AAPS PharmSciTech. 2013; 14(1):445–55.
29. Khanolkar A, Thorat V, Raut P, Samanta G. Application of Quality by Design: Development to Manufacturing of Diclofenac Sodium Topical Gel. AAPS PharmSciTech AAPS PharmSciTech 2017; 18(7):2754–63.